Bit and Power Loading for OFDM-Based Three-Node Relaying Communications

Yi Ma, *Member, IEEE*, Na Yi, *Student Member, IEEE*, and Rahim Tafazolli

***Abstract*—Bit and power loading (BPL) techniques have been intensively investigated for the single-link communications. In this paper, we propose a margin-adaptive BPL approach for orthogonal frequency-division multiplexing (OFDM) systems assisted by a single cooperative relay. This orthogonal half-duplex relay operates either in the selection detection-and-forward (SDF) mode or in the amplify-and-forward (AF) mode. Maximum-ratio combining is employed at the destination to attain the achievable distributed spatial diversity-gain. Assuming perfect channel knowledge is available at all nodes, the proposed approach is to minimize the transmit-power consumption at the target throughput (average number of bits/symbol) and the target link performance. With respect to various power-constraint conditions, we investigate two distributed resource-allocation strategies, namely flexible power ratio (FLPR) and fixed power ratio (FIPR). The FLPR strategy is proposed for scenarios without individual local power constraint. The source power and relay power have a flexible ratio for each subcarrier. The FIPR strategy is proposed for scenarios with individual local power constraint. The source power and relay power have a fixed ratio for each subcarrier. Computer simulations are carried out to evaluate the proposed approach with respect to the relay location. Significant performance improvement is observed in terms of both the symbol-error-rate and the transmit-power efficiency.**

***Index Terms*—Amplify-and-forward (AF), bit and power loading (BPL), detection-and-forward, orthogonal frequency-division multiplexing (OFDM), relay.**

I. Introduction

EMERGING wireless applications such as wireless multihop networks and mesh networks have an increasing demand for high spectral-efficiency and quality-of-service. However, the networking performance can be limited by diverse quality of wireless channels amongst distributed nodes. The performance can be significantly improved if distributed nodes can efficiently share their local radio resources. This has motivated significant research activity towards what is called cooperative communications or cooperative relaying technologies (e.g., [1], [2]). The basic structure for cooperative communications is the three-node relaying network accommodating one source, one relay, and one destination [3]. The relay often operates in the half-duplex mode. It can retransmit the received information by employing some relaying protocols such as detection-and-forward (DF), amplify-and-forward (AF), compress-and-forward, etc. (e.g., [4], [5]). The destination can employ maximum-ratio combining (MRC) of the received signals to achieve the maximum distributed spatial diversity-gain. Moreover, Chen and Laneman have proposed a piecewise-linear combining scheme to offer the near-optimum performance for noncoherent cooperative communications [6], [7]. Recently, European Commission has been considering to apply the cooperative relaying concept in the future high-data-rate cellular services (e.g., [8], [9]). The relaying node can either be a fixed relaying station or a low-mobility user [10]. This can combine the merits of the cooperative relaying technique with the advanced air-interface such as orthogonal frequency-division multiplexing (OFDM). Then, one of interesting research issues is to investigate the bit and power loading (BPL) technologies for the OFDM-based cooperative communications.

The BPL techniques have been intensively investigated for the single-link communications. They use the channel feedback to determine the number of bits per symbol and the required power for each subchannel in a parallel set of subchannels. The water-filling algorithm turns out to be the optimum BPL approach. However, this optimum approach may result in fractional number of bits/symbol, which can complicate encode/decoder (or modulation/demodulation) implementation. Practically, one can employ two well-known suboptimum BPL approaches, i.e., the margin-adaptive algorithm and the rate-adaptive algorithm, to offer the near water-filling solution and the integer number of bits/symbol [11], [12]. Specifically, the margin-adaptive approach is to minimize the transmit power subject to the target number of bits per block and the target link performance. This approach has received considerable applications in the OFDM systems. For instance, Wong *et al.* have investigated the margin-adaptive approach for the OFDM-FDMA systems [13]. Their investigation has included the single-user link adaptation and the multi-user resource competition. The rate-adaptive approach is to maximize the number of bits per block subject to the fixed transmit-power and the target link performance. This approach has also received considerable applications in the OFDM systems (e.g., [14]).

In this paper, we investigate the margin-adaptive BPL approach for the OFDM-based three-node relaying communications. The orthogonal half-duplex relay can employ either the symbol-level-selection (SLS) DF protocol or the AF protocol for retransmission. MRC is employed at the destination to maximize the received signal-to-noise ratio (SNR). Assuming perfect channel knowledge is available at all nodes, the proposed approach is to improve the transmit-power efficiency for the distributed senders. With respect to various

Manuscript received August 30, 2006; revised February 14, 2007, September 8, 2007 and November 15, 2007. The Associate Editor coordinating the review of this paper and approving it for publication was Prof. Qing Zhao. This work has been performed in the framework of European Commission IST project IST-4-027756 WINNER II, which was supported in part by the European Union. The work of N. Yi was supported in part by U.K. MVCE Core 4, which is suported in part by EPSRC.

The authors are with Centre for Communication Systems Research, the University of Surrey, Surrey GU2 7XH, U.K. (e-mail: y.ma@surrey.ac.uk).

Digital Object Identifier 10.1109/TSP.2008.920493

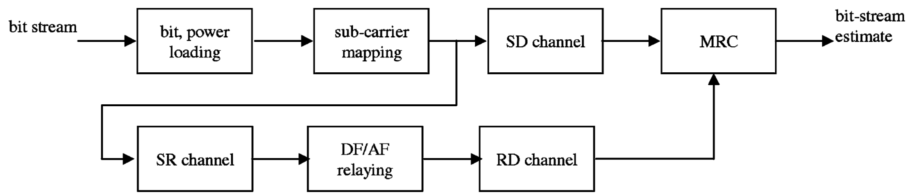

Fig. 1. Block diagram of the OFDM-based three-node relaying communication.

power-consumption conditions, we propose two distributed resource-allocation strategies, namely flexible power ratio (FLPR) and fixed power ratio (FIPR). The FLPR strategy is proposed for scenarios without individual local power constraint. For example, an access point (source) communicates to an user terminal with the help of a relaying station. Both the source and the relay can provide the required power to achieve the target performance. In this case, the source and relay have an optimum (or suboptimum) distributed power allocation for each subcarrier. The total transmit-power is optimally (or suboptimally) allocated between the source and relay. However, in many cases, the distributed senders have their individual power constrained, which cannot fulfill the optimum (or suboptimum) distributed power allocation required by the FLPR strategy. For example, a mobile relay might not be able to offer the sufficient power to support the FLPR strategy. In this case, we can employ the FIPR strategy, i.e., the source power and relay power have a fixed ratio for each subcarrier. This approach reduces the degree of freedom and offers a suboptimum solution to the problem that controls the power expended by each sender.

Note 1: Our performance investigation is focused on the amount by which the proposed approaches can reduce the required transmit-power. The investigation is carried out by examining the average power-consumption per bit. This method has been employed for evaluating cost efficiency of an adaptive transmission system (e.g., [13]).

Note 2: The proposed BPL approaches are optimized for the uncoded source. Certainly, employing error-control-codes can improve the link performance for adaptive transmissions [15], [16]. However, investigating BPL for coded-OFDM systems should take into account the impact of time-frequency correlation. This can significantly complicate the theoretical analysis.

The rest of this paper is organized as follows. Section II presents the OFDM-based three-node relaying communication. The margin-adaptive algorithm for the end-to-end communication is also introduced. Section III presents the proposed BPL approach for the SLS-DF relaying protocol. Section IV provides the investigation for the AF relaying protocol. Simulation results and discussions are given in Section V. Section VI draws the conclusion.

Notations: Throughout this paper, lower case boldface symbols are used to denote column vectors (e.g., $\boldsymbol{a}$) while upper case boldface symbols are used to denote matrices (e.g., $\mathbf{A}$). Elements of vectors or matrices are expressed as a_m or $A_{n,m}$. $\mathbf{I}_M$ denotes the identity matrix of size M. $|\mathbf{A}|$ denotes a matrix formed by the amplitude of the corresponding elements in $\mathbf{A}$. $\mathbf{D}(\boldsymbol{a})$ denotes a diagonal matrix with $\boldsymbol{a}$ in its diagonal. $(\cdot)^{\mathrm{T}}$, $(\cdot)^{\mathcal{H}}$, $(\cdot)^{\dagger}$ denotes the matrix transpose, Hermitian, and pseudo inverse, respectively. The superscripts $(\cdot)^{(\mathrm{s})}$, $(\cdot)^{(\mathrm{r})}$, $(\cdot)^{(\mathrm{d})}$, $(\cdot)^{(\mathrm{sd})}$, $(\cdot)^{(\mathrm{sr})}$, and $(\cdot)^{(\mathrm{rd})}$ denotes source, relay, destination, source-destination (SD) link, source-relay (SR) link, and relay-destination (RD) link, respectively.

II. System Model and Preparation

A. OFDM-Based Relaying Communications

The OFDM system has been well documented in the literature (e.g., [17]). The major idea is to transmit the information-bearing symbols over a number of low-rate orthogonal subcarriers. This is established by employing inverse discrete Fourier-transform (IDFT) at the transmitter and DFT at the receiver. A cyclic prefix (CP) is employed for introducing the channel circulant property and mitigating the inter-block interference. The above signal processing can effectively turn the frequency-selective channel into a number of parallel flat subchannels. The channel equalization and symbol detection can be performed in the frequency-domain. To simplify the presentation, we will only consider the frequency-domain signal representation in this paper.

Fig. 1 depicts the block diagram for the OFDM-based three-node relaying communications. Prior to transmission, the information-bearing bits are first fed into the BPL component to produce an $M\times 1$ symbol block $\boldsymbol{c}^{(\mathrm{s})}=[c_0^{(\mathrm{s})},c_1^{(\mathrm{s})},\cdots,c_{M-1}^{(\mathrm{s})}]^{\mathrm{T}}$, where c stands for the information-bearing symbol (with the variance $\sigma_c^2 = 1$) or zero symbol. These symbols are then modulated onto M corresponding subcarriers with the transmit power $\boldsymbol{\varepsilon}^{(\mathrm{s})} = [\varepsilon_0^{(\mathrm{s})},\varepsilon_1^{(\mathrm{s})},\cdots,\varepsilon_{M-1}^{(\mathrm{s})}]^{\mathrm{T}}$, where ε denotes the transmit power for each subcarrier. This block goes through the SD channel and the SR channel, respectively. Denoting $\boldsymbol{h}$ to be the channel coefficients on subcarriers, the received frequency-domain block at the destination and at the relay is expressible as

$$\text{SD link}:\quad \boldsymbol{y}^{(\mathrm{sd})}=\mathbf{D}\left(\boldsymbol{h}^{(\mathrm{sd})}\right)\mathbf{D}\left(\sqrt{\boldsymbol{\varepsilon}^{(\mathrm{s})}}\right)\boldsymbol{c}^{(\mathrm{s})}+\boldsymbol{v}^{(\mathrm{sd})} \quad (1)$$

$$\text{SR link}:\quad \boldsymbol{y}^{(\mathrm{sr})}=\mathbf{D}\left(\boldsymbol{h}^{(\mathrm{sr})}\right)\mathbf{D}\left(\sqrt{\boldsymbol{\varepsilon}^{(\mathrm{s})}}\right)\boldsymbol{c}^{(\mathrm{s})}+\boldsymbol{v}^{(\mathrm{sr})} \quad (2)$$

where $\boldsymbol{v}$ denotes the white Gaussian noise with zero mean and variance $\mathcal{N}_o$. The cooperative relay operates in the orthogonal half-duplex mode. After a certain signal processing, it can send an information-bearing block $\boldsymbol{c}^{(\mathrm{r})}$ to the destination through the RD channel. Then, the destination can receive the second version of the information as below

$$\text{RD link}:\quad \boldsymbol{y}^{(\mathrm{rd})}=\mathbf{D}\left(\boldsymbol{h}^{(\mathrm{rd})}\right)\boldsymbol{c}^{(\mathrm{r})}+\boldsymbol{v}^{(\mathrm{rd})}. \quad (3)$$

The format of $\boldsymbol{c}^{(\mathrm{r})}$ is related to the specific relaying protocols.

This system description is based on the typical setup for the relaying communications (e.g., in [1] and [10]). Recently, it has been reported (e.g., in [18]) that the nonorthogonal half-duplex relays are employed in order to exploit the potential spatial multiplexing-gain, i.e., both the source and the relays can send the information at the same time/frequency slot. However, this system setup results in different resource allocation strategy. Here, our investigation is carried out only for the typical setup introduced in Section II-A.

B. The SLS-DF Protocol

The selection DF relay has two typical protocols, i.e., frame-level-selection (FLS) DF and SLS-DF. In the FLS-DF protocol, the relay forwards every correctly received frame to the destination. In the SLS-DF protocol, the relay forwards every correctly received (or reliable) symbol to the destination. Recently, the SLS-DF protocol has received considerable attention for cooperative communications (e.g., [19]–[22]). This is because the SLS-DF protocol can offer the significant performance improvement in comparison with the FLS-DF protocol [22]. Basically, the SLS-DF protocol has two modes, i.e., ideal mode or outage mode. In the ideal mode, the relay should be capable of symbol error detection. This demands employment of CRC codes on the symbol level, which cannot be practically implemented [23]. In the outage mode, the relay can compute the received SNR for each subcarrier. When the received SNR is not smaller than a SNR threshold γ_{t}, the relay can forward the detected symbols to the destination. Sadek *et al.* have experimentally shown that the outage SLS-DF can offer very close performance to the ideal SLS-DF for the nonadaptive transmissions [22]. To clarify the presentation, here, we take the ideal mode as an example to introduce the SLS-DF protocol.

The ideal SLS-DF relay can relate the output $\boldsymbol{c}^{(\mathrm{r})}$ to $\boldsymbol{c}^{(\mathrm{s})}$ as below

$$\boldsymbol{c}^{(\mathrm{r})} = \mathbf{D}\left(\sqrt{\boldsymbol{\varepsilon}^{(\mathrm{r})}}\right)\boldsymbol{c}^{(\mathrm{s})}. \tag{4}$$

The vector $\boldsymbol{\varepsilon}^{(\mathrm{r})}$ can have zero elements corresponding to the unforwarded symbols or zero symbols. Define an $M\times M$ diagonal matrix $\boldsymbol{\Lambda} = [\mathbf{D}(\sqrt{\boldsymbol{\varepsilon}^{(\mathrm{r})}})]^{\dagger}\mathbf{D}(\sqrt{\boldsymbol{\varepsilon}^{(\mathrm{r})}})$. The destination can employ MRC of $\boldsymbol{y}^{(\mathrm{sd})}$ and $\boldsymbol{y}^{(\mathrm{rd})}$ to yield

$$\boldsymbol{y}^{(\mathrm{d})} = \mathbf{D}(\mathbf{w}_1)\boldsymbol{y}^{(\mathrm{sd})} + \mathbf{D}(\mathbf{w}_2)\boldsymbol{\Lambda}\boldsymbol{y}^{(\mathrm{rd})} \tag{5}$$

where $\mathbf{w}_1$, $\mathbf{w}_2$ denotes the MRC coefficients. Then, the single-tap equalizers, e.g., zero-forcing (ZF) or minimum mean-square error (MMSE) [24], can be employed for the channel equalization. These equalizers do not affect the SNR of the received symbols. The symbol detection performance is related to the effective SNR (denoted by $\boldsymbol{\gamma}^{(\mathrm{d})}$) for the MRC [25], i.e.,

$$\begin{aligned}\boldsymbol{\gamma}^{(\mathrm{d})} &= \boldsymbol{\gamma}^{(\mathrm{sd})} + \boldsymbol{\gamma}^{(\mathrm{rd})},\\ &= \frac{1}{\mathcal{N}_o}\left(\left|\mathbf{D}\left(\boldsymbol{h}^{(\mathrm{sd})}\right)\right|^2\boldsymbol{\varepsilon}^{(\mathrm{s})} + \left|\mathbf{D}\left(\boldsymbol{h}^{(\mathrm{rd})}\right)\right|^2\boldsymbol{\varepsilon}^{(\mathrm{r})}\right).\end{aligned} \tag{6}$$

For the N-ary quadrature-amplitude-modulation (QAM), the symbol-error-rate (SER) (denoted by $\mathcal{P}$) for the mth element of $\boldsymbol{y}^{(\mathrm{d})}$ is tightly upper-bounded by [24]

$$\mathcal{P}_m^{(\mathrm{d})} = 4\mathcal{Q}\left(\sqrt{\frac{3\gamma_m^{(\mathrm{d})}}{N-1}}\right) \tag{7}$$

where $\mathcal{Q}(\cdot)$ is the Gaussian Q-function.

C. The AF Protocol

In the AF protocol, the relay forwards all received noisy symbols with power re-allocation. Hence, the AF relay relates the output $\boldsymbol{c}^{(\mathrm{r})}$ to $\boldsymbol{c}^{(\mathrm{s})}$ as below

$$\begin{aligned}\boldsymbol{c}^{(\mathrm{r})} &= \mathbf{D}(\sqrt{\boldsymbol{\beta}})\boldsymbol{y}^{(\mathrm{sr})} &(8)\\ &= \mathbf{D}(\sqrt{\boldsymbol{\beta}})\mathbf{D}\left(\boldsymbol{h}^{(\mathrm{sr})}\right)\mathbf{D}\left(\sqrt{\boldsymbol{\varepsilon}^{(\mathrm{s})}}\right)\boldsymbol{c}^{(\mathrm{s})} + \mathbf{D}(\sqrt{\boldsymbol{\beta}})\boldsymbol{v}^{(\mathrm{sr})} &(9)\end{aligned}$$

where $\boldsymbol{\beta}$ denotes the amplifying coefficients. We can plug (9) into (3) and obtain

$$\begin{aligned}\boldsymbol{y}^{(\mathrm{rd})} = {}&\mathbf{D}\left(\boldsymbol{h}^{(\mathrm{rd})}\right)\mathbf{D}(\sqrt{\boldsymbol{\beta}})\mathbf{D}\left(\boldsymbol{h}^{(\mathrm{sr})}\right)\mathbf{D}\left(\sqrt{\boldsymbol{\varepsilon}^{(\mathrm{s})}}\right)\boldsymbol{c}^{(\mathrm{s})}\\ &+\mathbf{D}\left(\boldsymbol{h}^{(\mathrm{rd})}\right)\mathbf{D}(\sqrt{\boldsymbol{\beta}})\boldsymbol{v}^{(\mathrm{sr})} + \boldsymbol{v}^{(\mathrm{rd})}.\end{aligned} \tag{10}$$

The following operation is performed on $\boldsymbol{y}^{(\mathrm{rd})}$ to unify the noise variance to $\mathcal{N}_o$:

$$\bar{\boldsymbol{y}}^{(\mathrm{rd})} = \underbrace{\left(\left|\mathbf{D}\left(\boldsymbol{h}^{(\mathrm{rd})}\right)\mathbf{D}(\sqrt{\boldsymbol{\beta}})\right|^2 + \mathbf{I}_M\right)^{-\frac{1}{2}}}_{=\boldsymbol{\Theta}}\boldsymbol{y}^{(\mathrm{rd})}. \tag{11}$$

The destination can perform the MRC on $\boldsymbol{y}^{(\mathrm{sd})}$ and $\bar{\boldsymbol{y}}^{(\mathrm{rd})}$. The effective SNR $\boldsymbol{\gamma}^{(\mathrm{d})}$ can be calculated as

$$\begin{aligned}\boldsymbol{\gamma}^{(\mathrm{d})} = \frac{1}{\mathcal{N}_o}&\left(\left|\mathbf{D}\left(\boldsymbol{h}^{(\mathrm{sd})}\right)\right|^2\right.\\ &\left.+\left|\boldsymbol{\Theta}\mathbf{D}\left(\boldsymbol{h}^{(\mathrm{rd})}\right)\mathbf{D}(\sqrt{\boldsymbol{\beta}})\mathbf{D}\left(\boldsymbol{h}^{(\mathrm{sr})}\right)\right|^2\right)\boldsymbol{\varepsilon}^{(\mathrm{s})}.\end{aligned} \tag{12}$$

The SER for each subcarrier is tightly upper-bounded by (7).

D. Margin-Adaptive BPL for SD Communication

The margin-adaptive approach for the single-antenna single-link OFDM communications can be found in many literatures, e.g., Chow's algorithm and Levin-Campello algorithm [11]. The basic structure can be described as follows [13]. Consider $\overline{\mathcal{P}}$ to be the target SER on the mth subcarrier.[1] Loading the amount of b_m bits on the mth subcarrier with N-QAM ($N = 2^{b_m}$) needs the target SNR (denoted by $\bar{\gamma}$) as [derived from (7)]

$$\bar{\gamma}_m = \frac{1}{3}\left[\mathcal{Q}^{-1}(\overline{\mathcal{P}}/4)\right]^2(2^{b_m} - 1). \tag{13}$$

[1]Similar to the consideration in [13], we also fix the target SER $\overline{\mathcal{P}}$ for each subcarrier. Certainly, the target SER could be different for each subcarrier, i.e., $\overline{\mathcal{P}}_m$ and $\overline{\mathcal{P}} = (1/M)\sum_{m=0}^{M-1}\overline{\mathcal{P}}_m$. However, it can be easily justified that the later one offers larger block-error-rate than the considered target-SER setup. Therefore, the considered target-SER is important when the ARQ scheme requires retransmission of the whole block.

The BPL algorithm aims to minimize the total power cost for a system that transmits at a rate of B bits per block and achieves the target SER, $\overline{\mathcal{P}}$. This can be realized by minimizing the Lagrangian

$$\mathcal{L} = \sum_{m=0}^{M-1} \varepsilon_m + \rho\left(\sum_{m=0}^{M-1} b_m - B\right) \tag{14}$$

where ε_m is the transmit-power on the mth subcarrier, and ρ the Lagrangian multiplier for the constraint $\sum_{m=0}^{M-1} b_m - B = 0$. It can be shown that ε_m is a convex and increasing function of b_m. Thus, (14) can lead to the following BPL algorithm.

Initialization:

For all m, let $i = 0$ (iteration index), $b_m = 0$,

$\varepsilon_{0,m} = 0$, $\Delta\varepsilon_{i,m} = \varepsilon_{i,m} - \varepsilon_{i-1,m}$;

Bit-loading iterations:

Repeat the following B times:

$i = i + 1$;

$\hat{m} = \arg\min_m \Delta\varepsilon_{i-1,m}$;

$\varepsilon_{i,\hat{m}} = \varepsilon_{i-1,\hat{m}} + \Delta\varepsilon_{i,\hat{m}}$;

$b_{\hat{m}} = b_{\hat{m}} + 1$;

End.

Cioffi has mentioned in [11] that this is the best design for many transmission systems such as high data rate real-time communications, where variable data rate is not desirable. Moreover, our performance investigation is focused on the average power-consumption per bit. Then, the margin-adaptive approach can easily enable the fair comparison between the adaptive transmissions and the nonadaptive transmissions.

III. BPL FOR THE SLS-DF PROTOCOL

In this section, we investigate the BPL approach for both the ideal SLS-DF protocol and the outage SLS-DF protocol. Although the ideal SLS-DF protocol cannot be practically implemented, we can use it for the performance comparison with the outage SLS-DF protocol.

A. Ideal SLS-DF Protocol

Equations (5) and (6) indicate that the effective SNR for each subcarrier depends on whether the relay detects the symbol correctly. If the relay receives the correct symbol, which happens with probability $(1-\mathcal{P}_m^{(\mathrm{sr})})$, then the effective SNR for the mth subcarrier is $\gamma_m^{(\mathrm{d})} = \gamma_m^{(\mathrm{mrc})} = \gamma_m^{(\mathrm{sd})} + \gamma_m^{(\mathrm{rd})}$. Otherwise, the effective SNR is the SNR for the SD channel, i.e., $\gamma_m^{(\mathrm{d})} = \gamma_m^{(\mathrm{sd})}$. Hence, the SER at the destination is tightly upper bounded by

$$\mathcal{P}_m^{(\mathrm{d})} = 4\mathcal{Q}\left(\sqrt{\frac{3\gamma_m^{(\mathrm{mrc})}}{N-1}}\right)\left(1-\mathcal{P}_m^{(\mathrm{sr})}\right) + 4\mathcal{Q}\left(\sqrt{\frac{3\gamma_m^{(\mathrm{sd})}}{N-1}}\right)\mathcal{P}_m^{(\mathrm{sr})}. \tag{15}$$

Based on the fact $1 - \mathcal{P}_m^{(\mathrm{sr})} \leqslant 1$, we can further obtain the following upper bound:

$$\mathcal{P}_m^{(\mathrm{d})} \leqslant 4\mathcal{Q}\left(\sqrt{\frac{3\gamma_m^{(\mathrm{mrc})}}{N-1}}\right) + 16\mathcal{Q}\left(\sqrt{\frac{3\gamma_m^{(\mathrm{sd})}}{N-1}}\right)\mathcal{Q}\left(\sqrt{\frac{3\gamma_m^{(\mathrm{sr})}}{N-1}}\right). \tag{16}$$

A sufficient condition for the target SER to be achieved is for the upper bound in (16) to be no larger than the target SER, $\overline{\mathcal{P}}$. A sufficient condition for that to happen is

$$4\mathcal{Q}\left(\sqrt{\frac{3\gamma_m^{(\mathrm{mrc})}}{N-1}}\right) \leqslant \overline{\mathcal{P}}/2 \tag{17}$$

$$16\mathcal{Q}\left(\sqrt{\frac{3\gamma_m^{(\mathrm{sd})}}{N-1}}\right)\mathcal{Q}\left(\sqrt{\frac{3\gamma_m^{(\mathrm{sr})}}{N-1}}\right) \leqslant \overline{\mathcal{P}}/2. \tag{18}$$

We can see that the left hand of (18) (i.e., $\mathcal{P}_m^{(\mathrm{sd})}\mathcal{P}_m^{(\mathrm{sr})}$) is a monotonically decreasing function of the source power $\varepsilon_m^{(\mathrm{s})}$. Therefore, the minimum of source power (denoted by $\varepsilon_{m,\min}^{(\mathrm{s})}$) is unique, and can be found by employing the line search method [26]. For example, we can first use the Chernoff bound [24] to derive the following inequality:

$$\mathcal{P}_m^{(\mathrm{sd})}\mathcal{P}_m^{(\mathrm{sr})} \leqslant 16 \cdot \exp\left(-\frac{3\left(\gamma_m^{(\mathrm{sd})} + \gamma_m^{(\mathrm{sr})}\right)}{2(N-1)}\right). \tag{19}$$

Based on (18) and (19), we can easily find the following result:

$$0 < \varepsilon_{m,\min}^{(\mathrm{s})} \leqslant \frac{2 \cdot (2^{b_m} - 1)\mathcal{N}_o}{3 \cdot \left(\left|h_m^{(\mathrm{sd})}\right|^2 + \left|h_m^{(\mathrm{sr})}\right|^2\right)} \ln\left(\frac{32}{\overline{\mathcal{P}}}\right). \tag{20}$$

Then, the line search can be carried out within this range. When the source power $\varepsilon_m^{(\mathrm{s})}$ is determined, we can use (17) to obtain the relay power (22). To help our further investigation, we summarize the above results as below.

Theorem 1: Given the target SER, $\overline{\mathcal{P}}$, and the number of bits/symbol, b_m, a sufficient condition on the distributed power allocation on the mth subcarrier for the target SER to be satisfied is

$$\varepsilon_m^{(\mathrm{s})} \geqslant \varepsilon_{m,\min}^{(\mathrm{s})} \tag{21}$$

$$\varepsilon_m^{(\mathrm{r})} \geqslant \frac{(2^{b_m} - 1)\mathcal{N}_o}{3\left|h_m^{(\mathrm{rd})}\right|^2}\left[\mathcal{Q}^{-1}\left(\frac{\overline{\mathcal{P}}}{8}\right)\right]^2 - \frac{\varepsilon_m^{(\mathrm{s})} \cdot \left|h_m^{(\mathrm{sd})}\right|^2}{\left|h_m^{(\mathrm{rd})}\right|^2}. \tag{22}$$

Next, our objective is to minimize the power sum $\mathcal{E}_m = \varepsilon_m^{(\mathrm{s})} + \varepsilon_m^{(\mathrm{r})}$ for the mth subcarrier. This issue will be carefully investigated for both the FLPR and the FIPR scenarios.

1) The FLPR Strategy: This strategy is used to minimize the power sum $\mathcal{E}_m$ for the scenarios without individual local power constraint. We can first set the transmit-power $\varepsilon_m^{(\mathrm{s})}$, $\varepsilon_m^{(\mathrm{r})}$ to the lower bound for (21) and (22). According to Theorem 1, this power allocation can achieve the target SER. Then, we increase the source power with the difference $\delta^{(\mathrm{s})}$, i.e.,

$\varepsilon_m^{(\mathrm{s})} = \varepsilon_{m,\min}^{(\mathrm{s})} + \delta^{(\mathrm{s})}$. The lower bound for (22) indicates that the required relay power is reduced with the difference $\delta^{(\mathrm{r})} = -(\delta^{(\mathrm{s})}|h_m^{(\mathrm{sd})}|^2)/(|h_m^{(\mathrm{rd})}|^2)$. Then, the total power change for the mth subcarrier is

$$\Delta\mathcal{E}_m = \delta^{(\mathrm{s})} + \delta^{(\mathrm{r})} = \frac{\delta^{(\mathrm{s})}\left(\left|h_m^{(\mathrm{rd})}\right|^2 - \left|h_m^{(\mathrm{sd})}\right|^2\right)}{\left|h_m^{(\mathrm{rd})}\right|^2}. \quad (23)$$

Hence, the total power consumption for the mth subcarrier can be reduced (i.e., $\Delta\mathcal{E}_m < 0$) with increasing the source power only for the case $|h_m^{(\mathrm{rd})}| < |h_m^{(\mathrm{sd})}|$. In this case, the source should pay all power cost for this subcarrier. For the case of $|h_m^{(\mathrm{rd})}| > |h_m^{(\mathrm{sd})}|$, we should keep the initial power allocation, i.e., $\delta^{(\mathrm{s})} = 0$. For the special case $|h_m^{(\mathrm{rd})}| = |h_m^{(\mathrm{sd})}|$, we suggest the source pay all power cost. This can increase the SD link reliability. As a conclusion, the above statements can be summarized as below.

Corollary 1.1: Given the sufficient condition (21) and (22), for the case $|h_m^{(\mathrm{sd})}| \geqslant |h_m^{(\mathrm{rd})}|$, the power sum $\mathcal{E}_m$ is minimized with the following distributed power allocation:

$$\varepsilon_m^{(\mathrm{s})} = \frac{(2^{b_m}-1)\mathcal{N}_o}{3\left|h_m^{(\mathrm{sd})}\right|^2}\left[\mathcal{Q}^{-1}\left(\frac{\overline{\mathcal{P}}}{4}\right)\right]^2, \quad \varepsilon_m^{(\mathrm{r})} = 0. \quad (24)$$

Otherwise, the power sum $\mathcal{E}_m$ is minimized by employing the lower bound for (21) and (22).

2) The FIPR Strategy: In many cases, the distributed senders have their individual power constraint. Usually, this power constraint does not support the FLPR strategy. In this scenario, we can fix the power ratio for each subcarrier, i.e., $(\varepsilon_m^{(\mathrm{r})})/(\varepsilon_m^{(\mathrm{s})}) = (\mathcal{E}^{(\mathrm{r})})/(\mathcal{E}^{(\mathrm{s})}) = \eta$, where $\mathcal{E}^{(\mathrm{r})}, \mathcal{E}^{(\mathrm{s})}$ denotes the power constraint for the relay and the source, respectively. This is a sufficient condition for the relay/source power balancing required, and the extra (subcarrier) constraint is for analytic simplicity.

Corollary 1.2: Given the sufficient condition (21) and (22) and the fixed power ratio, η, the minimum of total transmit-power for the mth subcarrier is

$$\min\left(\varepsilon_m^{(\mathrm{r})} + \varepsilon_m^{(\mathrm{s})}\right) = (1+\eta)\varepsilon_{m,\max}^{(\mathrm{s})} \quad (25)$$

where

$$\varepsilon_{m,\max}^{(\mathrm{s})} = \max\left(\varepsilon_{m,\min}^{(\mathrm{s})}, \frac{(2^{b_m}-1)\mathcal{N}_o}{3\left(\eta\left|h_m^{(\mathrm{rd})}\right|^2 + \left|h_m^{(\mathrm{sd})}\right|^2\right)} \times\left[\mathcal{Q}^{-1}\left(\frac{\overline{\mathcal{P}}}{8}\right)\right]^2\right). \quad (26)$$

The proof for this result is simple. We can first replace $\varepsilon_m^{(\mathrm{r})}$ with $\eta\varepsilon_m^{(\mathrm{s})}$ in (22) to obtain another lower bound for the source power (i.e., the second term at the right hand of (26)). As shown in (26), the source power should be the maximum of two lower bounds.

B. Outage SLS-DF Protocol

In this protocol, the relay can measure the received SNR for each subcarrier. When the received SNR is smaller than the SNR threshold[2] (i.e., $\gamma_m^{(\mathrm{sr})} < \gamma_{\mathrm{t},m}$), the relay does not transmit the received symbols on the mth subcarrier. In this case, the SER at the destination is $\mathcal{P}_m^{(\mathrm{d})} = \mathcal{P}_m^{(\mathrm{sd})}$. Otherwise, the relay transmits the received symbols on the mth subcarrier. Then, the SER at the destination is expressible as

$$\mathcal{P}_m^{(\mathrm{d})} = \mathcal{P}_m^{(\mathrm{sr}),\gamma_{\mathrm{t},m}}\mathcal{P}_m^{(\mathrm{mrc}),\gamma_{\mathrm{t},m}} + \left(1 - \mathcal{P}_m^{(\mathrm{sr}),\gamma_{\mathrm{t},m}}\right)\mathcal{P}_m^{(\mathrm{mrc})} \quad (27)$$

where $\mathcal{P}_m^{(\mathrm{sr}),\gamma_{\mathrm{t},m}}$ denotes the SER at the relay for $\gamma_m^{(\mathrm{sr})} \geqslant \gamma_{\mathrm{t},m}$, and $\mathcal{P}_m^{(\mathrm{mrc}),\gamma_{\mathrm{t},m}}$ the SER for the MRC in the presence of error propagation. Based on the fact $\mathcal{P}_m^{(\mathrm{mrc}),\gamma_{\mathrm{t},m}} \leqslant 1$ and $(1 - \mathcal{P}_m^{(\mathrm{sr}),\gamma_{\mathrm{t},m}}) \leqslant 1$, (27) is upper bounded by

$$\mathcal{P}_m^{(\mathrm{d})} \leqslant \mathcal{P}_m^{(\mathrm{sr}),\gamma_{\mathrm{t},m}} + \mathcal{P}_m^{(\mathrm{mrc})}. \quad (28)$$

As a summary of the above discussions, the SER at the destination can be upper bounded by

$$\mathcal{P}_m^{(\mathrm{d})} \leqslant S_m\mathcal{P}_m^{(\mathrm{sd})} + (1-S_m)\left(\mathcal{P}_m^{(\mathrm{sr}),\gamma_{\mathrm{t},m}} + \mathcal{P}_m^{(\mathrm{mrc})}\right) \quad (29)$$

where S_m is binary, i.e.,

$$S_m = \begin{cases} 1, & \gamma_m^{(\mathrm{sr})} < \gamma_{\mathrm{t},m}; \\ 0, & \gamma_m^{(\mathrm{sr})} \geqslant \gamma_{\mathrm{t},m}. \end{cases} \quad (30)$$

A sufficient condition for the target SER to be achieved is for the upper bound in (29) to be no larger than the target SER, $\overline{\mathcal{P}}$. For the case of $S_m = 0$, a sufficient condition for that to happen is: C1) $\mathcal{P}_m^{(\mathrm{mrc})} < (\overline{\mathcal{P}})/(2)$; C2) $\mathcal{P}_m^{(\mathrm{sr}),\gamma_{\mathrm{t},m}} < (\overline{\mathcal{P}})/(2)$. The condition C1) leads to the result (22). Based on the fact

$$\mathcal{P}_m^{(\mathrm{sr}),\gamma_{\mathrm{t},m}} \leqslant 4\mathcal{Q}\left(\sqrt{\frac{3\gamma_{\mathrm{t},m}}{N-1}}\right) \quad (31)$$

the following condition is demanded for protecting the condition C2), i.e.,

$$4\mathcal{Q}\left(\sqrt{\frac{3\gamma_{\mathrm{t},m}}{N-1}}\right) \leqslant \overline{\mathcal{P}}/2. \quad (32)$$

We can replace $\gamma_{\mathrm{t},m}$ in (32) with the SNR $(\varepsilon_m^{(\mathrm{s})}|h_m^{(\mathrm{sr})}|^2)/(\mathcal{N}_o)$ and obtain the following result:

$$\varepsilon_m^{(\mathrm{s})} \geqslant \frac{(2^{b_m}-1)\mathcal{N}_o}{3\left|h_m^{(\mathrm{sr})}\right|^2}\left[\mathcal{Q}^{-1}\left(\frac{\overline{\mathcal{P}}}{8}\right)\right]^2. \quad (33)$$

As a conclusion, we can summarize the above discussions as below.

Theorem 2: Given the target SER, $\overline{\mathcal{P}}$, and the number of bits/symbol, b_m, for the case $S_m = 0$, a sufficient condition on the distributed power allocation on the mth subcarrier for the target SER to be satisfied is (22) and (33).

[2]The SNR threshold $\gamma_{\mathrm{t},m}$ can be different with respect to the modulation order.

Now, we are ready to investigate the FLPR and FIPR strategy for the outage SLS-DF protocol.

1) The FLPR Strategy: Theorem 2 provides the sufficient condition only for the case $S_m = 0$. To protect this case, the condition (33) needs to be satisfied. However, the case $S_m = 1$ will happen under the following condition:

$$\varepsilon_m^{(\mathrm{s})} < \frac{(2^{b_m}-1)\mathcal{N}_o}{3\left|h_m^{(\mathrm{sr})}\right|^2}\left[\mathcal{Q}^{-1}\left(\frac{\overline{\mathcal{P}}}{8}\right)\right]^2. \tag{34}$$

In this case, the relay does not transmit on the mth subcarrier, i.e., $\varepsilon_m^{(\mathrm{r})} = 0$. The source should guarantee the condition $\mathcal{P}_m^{(\mathrm{sd})} \leqslant \overline{\mathcal{P}}$, which results in

$$\varepsilon_m^{(\mathrm{s})} \geqslant \frac{(2^{b_m}-1)\mathcal{N}_o}{3\left|h_m^{(\mathrm{sd})}\right|^2}\left[\mathcal{Q}^{-1}\left(\frac{\overline{\mathcal{P}}}{4}\right)\right]^2. \tag{35}$$

The conditions (34) and (35) can lead to the following results:

$$\frac{\left|h_m^{(\mathrm{sr})}\right|}{\left|h_m^{(\mathrm{sd})}\right|} < \frac{\mathcal{Q}^{-1}\left(\frac{\overline{\mathcal{P}}}{8}\right)}{\mathcal{Q}^{-1}\left(\frac{\overline{\mathcal{P}}}{4}\right)}. \tag{36}$$

We can easily justify that the right hand of (36) is very close to 1 for the target SER $\overline{\mathcal{P}} < 1 \times 10^{-2}$. Moreover, Corollary 1.1 shows that the source should pay all power cost under the condition $|h_m^{(\mathrm{sd})}| \geqslant |h_m^{(\mathrm{rd})}|$. This statement is derived from the condition (22), which is also valid for the outage SLS-DF protocol. Therefore, the FLPR strategy here should obey the following criterion.

Corollary 2.1: Given the sufficient condition (23) and (33), for the channel condition (36) and $|h_m^{(\mathrm{sd})}| \geqslant |h_m^{(\mathrm{rd})}|$, the power sum $\mathcal{E}_m$ is minimized with the distributed power allocation as in (24). Otherwise, the power sum $\mathcal{E}_m$ is minimized by employing the lower bound for (22) and (33).

2) The FIPR Strategy: In this scenario, we only need to consider the case $S_m = 0$. This is to protect the fixed power ratio for each subcarrier. Therefore, the source power should simultaneously fulfill the condition (22) and (33). Then, the power allocation strategy can be described as below.

Corollary 2.2: Given the sufficient condition (22) and (33) and the fixed power ratio, η, the minimum of total transmit-power for the mth subcarrier is given by (25) with

$$\varepsilon_{m,\max}^{(\mathrm{s})} = \max\left(\frac{(2^{b_m}-1)\mathcal{N}_o}{3\left|h_m^{(\mathrm{sr})}\right|^2}\left[\mathcal{Q}^{-1}\left(\frac{\overline{\mathcal{P}}}{8}\right)\right]^2, \frac{(2^{b_m}-1)\mathcal{N}_o}{3\left(\eta\left|h_m^{(\mathrm{rd})}\right|^2+\left|h_m^{(\mathrm{sd})}\right|^2\right)}\left[\mathcal{Q}^{-1}\left(\frac{\overline{\mathcal{P}}}{8}\right)\right]^2\right). \tag{37}$$

So far, we have investigated the BPL criteria for the SLS-DF protocols. The BPL approach can be implemented by modifying slightly the algorithm introduced in Section II-D.

Initialization:

For all m, let $i = 0$ (iteration index), $b_m = 0$,

$\mathcal{E}_{0,m} = 0$, $\Delta\mathcal{E}_{i,m} = \mathcal{E}_{i,m} - \mathcal{E}_{i-1,m}$;

Bit-loading iterations:

Repeat the following B times:

$i = i + 1$;

$\hat{m} = \arg\min_m \Delta\mathcal{E}_{i-1,m}$;

$\mathcal{E}_{i,\hat{m}} = \mathcal{E}_{i-1,\hat{m}} + \Delta\mathcal{E}_{i,\hat{m}}$;

Allocate $\mathcal{E}_{i,\hat{m}}$ between the source and relay;

$b_{\hat{m}} = b_{\hat{m}} + 1$;

End.

IV. BPL FOR THE AF PROTOCOL

In the AF protocol, the SER $\mathcal{P}_m^{(\mathrm{d})}$ is only related to the effective SNR after the MRC. Eqn. (12) shows that the effective SNR for the mth subcarrier is expressible as

$$\gamma_m^{(\mathrm{d})} = \frac{\varepsilon_m^{(\mathrm{s})}}{\mathcal{N}_o}\left(\left|h_m^{(\mathrm{sd})}\right|^2 + \frac{\left|h_m^{(\mathrm{rd})}\right|^2\left|h_m^{(\mathrm{sr})}\right|^2\beta_m}{\beta_m\left|h_m^{(\mathrm{rd})}\right|^2+1}\right). \tag{38}$$

The relay power and the source power for the mth subcarrier can be related as

$$\varepsilon_m^{(\mathrm{r})} = \beta_m\left|h_m^{(\mathrm{sr})}\right|^2\varepsilon_m^{(\mathrm{s})} + \beta_m\mathcal{N}_o. \tag{39}$$

Given the target SNR $\bar{\gamma}$ (corresponding to the target SER $\overline{\mathcal{P}}$), our objective is to minimize the power sum $\mathcal{E}_m = \varepsilon_m^{(\mathrm{s})} + \varepsilon_m^{(\mathrm{r})}$ for the mth subcarrier. Next, we will investigate this issue for the FLPR strategy and the FIPR strategy, respectively.

A. The FLPR Strategy

We can use (39) to obtain β_m as

$$\beta_m = \frac{\mathcal{E}_m - \varepsilon_m^{(\mathrm{s})}}{\left|h_m^{(\mathrm{sr})}\right|^2\varepsilon_m^{(\mathrm{s})} + \mathcal{N}_o}. \tag{40}$$

Plugging (40) into (38) yields

$$\gamma_m^{(\mathrm{d})} = \frac{\varepsilon_m^{(\mathrm{s})}}{\mathcal{N}_o}\left(\left|h_m^{(\mathrm{sd})}\right|^2 + \frac{\left|h_m^{(\mathrm{sr})}\right|^2\left|h_m^{(\mathrm{rd})}\right|^2(\mathcal{E}_m-\varepsilon_m^{(\mathrm{s})})}{\left(\left|h_m^{(\mathrm{sr})}\right|^2-\left|h_m^{(\mathrm{rd})}\right|^2\right)\varepsilon_m^{(\mathrm{s})}+\left|h_m^{(\mathrm{rd})}\right|^2\mathcal{E}_m+\mathcal{N}_o}\right). \tag{41}$$

It can be easily justified that $\gamma_m^{(\mathrm{d})}$ is a monotonically increasing function of the power sum $\mathcal{E}_m$. Assuming $\mathcal{E}_m$ to be determined, our objective is equivalent to finding an $\varepsilon_m^{(\mathrm{s})} \in (0, \mathcal{E}_m]$ corresponding to the maximum $\gamma_m^{(\mathrm{d})}$. Prior to solving this constrained optimization problem, we need to study the monotonicity of $\gamma_m^{(\mathrm{d})}$ with respect to $\varepsilon_m^{(\mathrm{s})}$ for the range of $\varepsilon_m^{(\mathrm{s})} \in (0, \mathcal{E}_m]$.

For the condition $(\partial\gamma_m^{(\mathrm{mrc})})/(\partial\varepsilon_m^{(\mathrm{s})}) > 0$, $\gamma_m^{(\mathrm{d})}$ is a monotonically increasing function of $\varepsilon_m^{(\mathrm{s})}$. This leads to the following result

$$f\left(\varepsilon_m^{(\mathrm{s})}\right) = A_m B_m \left(\varepsilon_m^{(\mathrm{s})}\right)^2 + 2A_m C_m \varepsilon_m^{(\mathrm{s})} + C_m D_m > 0 \quad (42)$$

where the coefficients A_m, B_m, C_m, D_m are defined as

$$A_m = \left|h_m^{(\mathrm{sd})}\right|^2 \left|h_m^{(\mathrm{sr})}\right|^2 - \left|h_m^{(\mathrm{sd})}\right|^2 \left|h_m^{(\mathrm{rd})}\right|^2 - \left|h_m^{(\mathrm{sr})}\right|^2 \left|h_m^{(\mathrm{rd})}\right|^2 \quad (43)$$

$$B_m = \left|h_m^{(\mathrm{sr})}\right|^2 - \left|h_m^{(\mathrm{rd})}\right|^2 \quad (44)$$

$$C_m = \left|h_m^{(\mathrm{rd})}\right|^2 \mathcal{E}_m + \mathcal{N}_o \quad (45)$$

$$D_m = \left|h_m^{(\mathrm{sd})}\right|^2 \left|h_m^{(\mathrm{rd})}\right|^2 \mathcal{E}_m + \left|h_m^{(\mathrm{sd})}\right|^2 \mathcal{N}_o + \left|h_m^{(\mathrm{sr})}\right|^2 \left|h_m^{(\mathrm{rd})}\right|^2 \mathcal{E}_m. \quad (46)$$

We can see that $f(\varepsilon_m^{(\mathrm{s})})$ is a second-order polynomial function, whose characteristic depends on the the coefficient $A_m B_m$ and the root distribution. This function has real roots under the following condition:

$$\Delta_m = 4A_m^2 C_m^2 - 4A_m B_m C_m D_m \geqslant 0. \quad (47)$$

Plugging (43)–(46) into (47) leads to the result $A_m \leqslant 0$. Based on the above analysis, we can obtain the following interesting results.

Lemma 1: Suppose $A_m \geqslant 0$. $\gamma_m^{(\mathrm{d})}$ is a monotonically increasing function for $\varepsilon_m^{(\mathrm{s})} \in (0, \mathcal{E}_m]$.

Proof: We can justify this result by considering two cases, i.e., $A_m = 0$ and $A_m > 0$. Due to $C_m D_m > 0$, the result (42) holds for the condition $A_m = 0$. The condition $A_m > 0$ results in

$$\left|h_m^{(\mathrm{sr})}\right|^2 > \left|h_m^{(\mathrm{rd})}\right|^2 + \frac{\left|h_m^{(\mathrm{sr})}\right|^2 \left|h_m^{(\mathrm{rd})}\right|^2}{\left|h_m^{(\mathrm{sd})}\right|^2} > \left|h_m^{(\mathrm{rd})}\right|^2. \quad (48)$$

In this case, (44) infers $B_m > 0$. Due to $\Delta_m < 0$ and $A_m B_m > 0$, the result (42) holds as well. This lemma is therefore proved. In this case, $\gamma_m^{(\mathrm{d})}$ can achieve its maximum at $\varepsilon_m^{(\mathrm{s})} = \mathcal{E}_m$.

Lemma 2: Suppose $A_m < 0$ and $B_m > 0$. Let ξ be the positive root for the equation $f(\varepsilon_m^{(\mathrm{s})}) = 0$. $\gamma_m^{(\mathrm{d})}$ achieves the maximum at $\varepsilon_m^{(\mathrm{s})} = \xi$ only when $|h_m^{(\mathrm{sd})}| < |h_m^{(\mathrm{rd})}|$ and

$$\frac{\mathcal{E}_m}{\mathcal{N}_o} > \frac{\left|h_m^{(\mathrm{sd})}\right|^2}{\left|h_m^{(\mathrm{sr})}\right|^2 \left(\left|h_m^{(\mathrm{rd})}\right|^2 - \left|h_m^{(\mathrm{sd})}\right|^2\right)}. \quad (49)$$

Otherwise, $\gamma_m^{(\mathrm{d})}$ achieves the maximum at $\varepsilon_m^{(\mathrm{s})} = \mathcal{E}_m$.

Proof: For the condition $A_m < 0$, the equation $f(\varepsilon_m^{(\mathrm{s})}) = 0$ has two real roots denoted by ξ_1 and ξ_2, respectively. The product of ξ_1 and ξ_2 is given by

$$\xi_1 \xi_2 = \frac{C_m D_m}{A_m B_m} < 0. \quad (50)$$

Hence, the equation $f(\varepsilon_m^{(\mathrm{s})}) = 0$ only has one positive root. Assuming ξ_2 to be the positive one, (42) holds only for $\varepsilon_m^{(\mathrm{s})} \in (0, \xi_2]$. In other words, $\gamma_m^{(\mathrm{d})}$ is a monotonically increasing function for $\varepsilon_m^{(\mathrm{s})} \in (0, \xi_2]$. Therefore, $\gamma_m^{(\mathrm{d})}$ can achieve the maximum at

$$\varepsilon_m^{(\mathrm{s})} = \min(\xi_2, \mathcal{E}_m). \quad (51)$$

As shown in Appendix A, $\min(\xi_2, \mathcal{E}_m) = \xi_2$ holds only for the conditions $|h_m^{(\mathrm{sd})}| < |h_m^{(\mathrm{rd})}|$ and (49).

Lemma 3: Suppose $A_m < 0$ and $B_m < 0$. Let ξ_1, ξ_2 be the roots for $f(\varepsilon_m^{(\mathrm{s})}) = 0$ $(\xi_1 < \xi_2)$. $\gamma_m^{(\mathrm{d})}$ achieves the maximum at $\varepsilon_m^{(\mathrm{s})} = \xi_1 < \mathcal{E}_m$ only for the conditions $|h_m^{(\mathrm{sd})}| < |h_m^{(\mathrm{rd})}|$ and (49). Otherwise, $\gamma_m^{(\mathrm{d})}$ achieves the maximum at $\varepsilon_m^{(\mathrm{s})} = \mathcal{E}_m$.

Proof: In this case, the equation $f(\varepsilon_m^{(\mathrm{s})}) = 0$ has two real roots. But, the product of two roots is positive, i.e., the sign for two roots is identical. Due to $A_m B_m > 0$, the minimum of $f(\varepsilon_m^{(\mathrm{s})})$ is negative and can be achieved at

$$\varepsilon_m^{(\mathrm{s})} = -\frac{C_m}{D_m} > 0. \quad (52)$$

It can be concluded that both roots are positive. The result (42) holds for $\varepsilon_m^{(\mathrm{s})} \in (0, \xi_1]$ or $\varepsilon_m^{(\mathrm{s})} \geqslant \xi_2$. Hence, $\gamma_m^{(\mathrm{d})}$ achieves the maximum at $\varepsilon_m^{(\mathrm{s})} = \xi_1$ for the range of $(0, \xi_2)$. On the other hand, $\gamma_m^{(\mathrm{d})}$ is monotonically increasing for $\varepsilon_m^{(\mathrm{s})} \geqslant \xi_2$. Hence, there exists a threshold $\xi_t (> \xi_2)$ fulfilling $\gamma_m^{(\mathrm{d})}(\xi_1) = \gamma_m^{(\mathrm{d})}(\xi_t)$. If $\mathcal{E}_m > \xi_t$, the maximum of $\gamma_m^{(\mathrm{d})}$ is achieved at $\varepsilon_m^{(\mathrm{s})} = \mathcal{E}_m$. The threshold ξ_t is derived in Appendix B.

Lemma 4: Suppose $A_m < 0$ and $B_m = 0$. $\gamma_m^{(\mathrm{d})}$ achieves the maximum at

$$\varepsilon_m^{(\mathrm{s})} = -\frac{D_m}{2A_m} \quad (53)$$

under the conditions (49) and $|h_m^{(\mathrm{sd})}| < |h_m^{(\mathrm{rd})}|$. Otherwise, $\gamma_m^{(\mathrm{d})}$ achieves the maximum at $\varepsilon_m^{(\mathrm{s})} = \mathcal{E}_m$.

Proof: See Appendix C.

As a summary of Lemmas. 1–4, we can conclude the following major result for the optimum power allocation.

Theorem 3: Define

$$\xi = \frac{-2A_m C_m - \sqrt{\Delta_m}}{2A_m B_m} \quad (54)$$

$$\xi_t = \frac{\left|h_m^{(\mathrm{sd})}\right|^2 \mathcal{N}_o}{\left|h_m^{(\mathrm{sr})}\right|^2 \left(\left|h_m^{(\mathrm{rd})}\right|^2 - \left|h_m^{(\mathrm{sd})}\right|^2\right)}. \quad (55)$$

The source power is $\varepsilon_m^{(\mathrm{s})} = \xi$ under the conditions: C3) $|h_m^{(\mathrm{sd})}| < |h_m^{(\mathrm{rd})}|$, and C4) $\mathcal{E}_m \in (\xi_t, (\overline{\gamma}\mathcal{N}_o)/(|h_m^{(\mathrm{sd})}|^2))$. Otherwise, the source power is $\varepsilon_m^{(\mathrm{s})} = \mathcal{E}_m$.

Proof: It can be easily justified that (54) is the desired root in Lemmas 1–3. Using the upper bound in C4), the SD link can achieve the target SNR $\overline{\gamma}$ without need of the relay. Others are all proved results.

Based on the above resource-allocation criterion, the BPL algorithm can be implemented as below.

Step 1: Use (13) to calculate the target SNR $\bar{\gamma}$;
Step 2: Calculating the range of $\mathcal{E}_m$ in C4);
Step 3: If C3), C4) holds, let $\varepsilon_m^{(\mathrm{s})} = \xi$.
Otherwise, let $\varepsilon_m^{(\mathrm{s})} = \mathcal{E}_m = \overline{\gamma}\mathcal{N}_o/|h_m^{(\mathrm{sd})}|^2$ and goto Step 5;
Step 4: Searching $\mathcal{E}_m$ over the range in C4) to minimize $|\gamma_m^{(\mathrm{d})} - \bar{\gamma}|$;
Step 5: Use the BPL algorithm in Section II-D to minimize $\sum_{m=0}^{M-1} \mathcal{E}_m$;
End;

Note 1: Since $\gamma_m^{(\mathrm{d})}$ is the monotonically increasing function of $\mathcal{E}_m$, we can employ the line search algorithm in Step 4. *Note 2*: Recently, optimal power allocation for the AF relaying channel has been reported in [27]. Differed from our approach, the reported scheme is based on the assumption of no SD link, and takes into account of the local power-constraint condition.[3] This effectively results in the different power-allocation strategy.

B. The FIPR Strategy

In the FIPR strategy, the transmit-power ratio on the mth subcarrier is fixed to

$$\eta = \beta_m \frac{\left|h_m^{(\mathrm{sr})}\right|^2 \varepsilon_m^{(\mathrm{s})} + \mathcal{N}_o}{\varepsilon_m^{(\mathrm{s})}}. \tag{56}$$

Applying (56) in (38) results in

$$\gamma_m^{(\mathrm{d})} = \frac{\varepsilon_m^{(\mathrm{s})}}{\mathcal{N}_o} \frac{\overline{A}_m \varepsilon_m^{(\mathrm{s})} + \left|h_m^{(\mathrm{sd})}\right|^2 \mathcal{N}_o}{\overline{B}_m \varepsilon_m^{(\mathrm{s})} + \mathcal{N}_o} \tag{57}$$

where

$$\overline{A}_m = \left|h_m^{(\mathrm{sd})}\right|^2 \left|h_m^{(\mathrm{rd})}\right|^2 \eta + \left|h_m^{(\mathrm{sd})}\right|^2 \left|h_m^{(\mathrm{sr})}\right|^2 + \left|h_m^{(\mathrm{rd})}\right|^2 \left|h_m^{(\mathrm{sr})}\right|^2 \eta \tag{58}$$

$$\overline{B}_m = \left|h_m^{(\mathrm{rd})}\right|^2 \eta + \left|h_m^{(\mathrm{sr})}\right|^2. \tag{59}$$

It is easy to justify that $\gamma_m^{(\mathrm{d})}$ is a monotonically increasing function of $\varepsilon_m^{(\mathrm{s})}$. Given the target SNR $\overline{\gamma}$, we can obtain the demanded $\varepsilon_m^{(\mathrm{s})}$ as

$$\varepsilon_m^{(\mathrm{s})} = \frac{\overline{B}_m\overline{\gamma} - \left|h_m^{(\mathrm{sd})}\right|^2 + \sqrt{\left(\overline{B}_m\overline{\gamma} - \left|h_m^{(\mathrm{sd})}\right|^2\right)^2 + 4\overline{A}_m\overline{\gamma}}}{2\overline{A}_m/\mathcal{N}_o}. \tag{60}$$

[3]It is very difficult to consider the optimum power-allocation strategy in the presence of SD link together with the local power-constraint condition.

Then, the BPL approach can be implemented as follows.

Step 1) Determine the minimum source-power $\varepsilon_m^{(\mathrm{s})}$ via (60), and calculate the minimum power sum $\min(\mathcal{E}_m) = (1+\eta)\varepsilon_m^{(\mathrm{s})}$ for a given η (e.g., $\eta = 1$);
Step 2) Use the BPL algorithm introduced in Section III-B to minimize $\sum_{m=0}^{M-1} \mathcal{E}_m$.

V. Simulation Results and Performance Evaluation

Computer simulations were used to examine the required transmit-power per bit and the final SER for both the SLS-DF and the AF-based three-node relaying communications. The results were obtained by averaging over 5 000 independent channel realizations. The linear MMSE method was employed for the channel equalization. Throughout the simulations, the BPL algorithms were optimized for the target SER 1×10^{-4}. Then, the link performance was examined by changing the noise power. The CP-OFDM system setup was given by (the typical setup for HIPERLAN/2 in [28]): $M = 64$ subcarriers, 8 samples in the CP. The OFDM block duration (exclusive CP) was 3.2 μs. Each burst consisted of 64 OFDM blocks. The information-bearing bits were randomly generated independent and equally likely. The number of bits per OFDM block was $B = 256$ bits.[4] The modulation schemes were N-QAM with $N = 4$, 16, 64, respectively. The channel impulse response for each link was generated according to the indoor channel model A specified by ETSI for HIPERLAN/2 [29]. The channel gain (denoted by G) for each link was considered as the following three cases:

	SD link	RD link	SR link
Case I :	$G = 1$	$G = 1$	$G = 10$
Case II :	$G = 1$	$G = 10$	$G = 1$
Case III :	$G = 1$	$G = 4$	$G = 4$

Cases I, II, and III are corresponding to the scenarios: the relay is close to source, close to the destination, and in the middle between the source and the destination, respectively. The simulations were divided into four experiments with respect to various BPL approaches and relaying protocols. We considered two baselines for the performance comparison. One was the nonadaptive 16QAM-OFDM relaying communication. The other was called the SD-adaptive case, i.e., the source performed the BPL approach based on the channel quality of the SD link, and sent the information in the broadcasting fashion. The relay retransmitted the received symbols according to the corresponding relaying protocols.

Experiment 1 (SLS-DF, FLPR): The objective of this experiment is to evaluate the proposed FLPR approaches for the outage SLS-DF relaying protocol. The SNR threshold is corresponding to the SER at relay (i.e., $\mathcal{P}^{(\mathrm{sr})} = 0.1$). We first examine the proposed BPL approach based on the outage behavior, i.e., the outage SLS (OSLS) approach addressed in Section III-B. Fig. 2 illustrates the SER at the destination as a function of the total transmit-power per bit to noise. It is observed that the OSLS approach can improve significantly the

[4]This setup was used to offer the fair comparison with the nonadaptive 16QAM-OFDM communications.

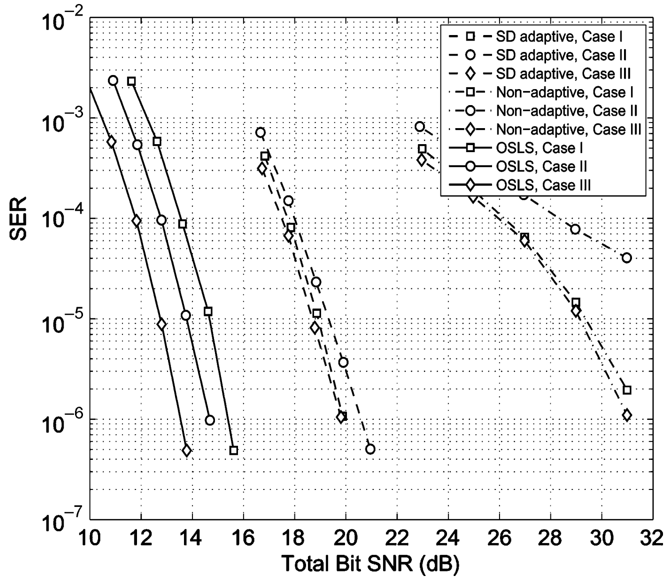

Fig. 2. SER versus total average bit SNR. A comparison amongst outage SLS-DF, SD adaptive only, and nonadaptive DF communications.

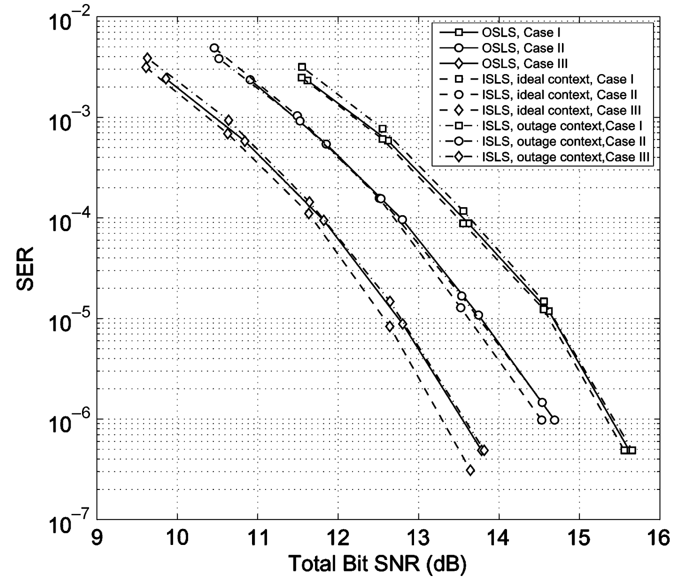

Fig. 3. SER versus total average bit SNR. A comparison amongst outage SLS-DF, ideal SLS-DF in ideal context, and ideal SLS-DF in outage context.

SER performance or the transmit-power efficiency in comparison to both baselines. Taking Case I and $\mathcal{P}^{(\mathrm{d})} = 1 \times 10^{-4}$ as an example, the OSLS approach shows about 12 dB gain and 4 dB gain in comparison to the nonadaptive case and the SD adaptive case, respectively. This result shows the significance of the multi-link adaptation. Fig. 2 also reflects another interesting phenomenon. For the nonadaptive approach, Case II shows the worst performance. Cases I and III have the very close SER. This is a well-known feature for the SDF relaying protocol [22]. It is observed that the SD-adaptive approach mitigates the difference amongst three cases. This is because the source is optimized for the SD link, which can reduce the impact of the relaying link on the final performance.

We then examine the proposed BPL approach originally optimized for the ideal SLS (ISLS) protocol. As shown in Section III-A, the BPL result only depends on the quality of relaying channels. Therefore, the ISLS approach can also be employed in the outage SLS-DF scenario. For example, the source can load the power and the bits according to the ISLS criterion. When the outage SLS-DF relay needs to forward the received symbol, the transmit-power should be in line with the ISLS criterion. Fig. 3 illustrates the SER performance for both the ideal SLS-DF protocol and the outage SLS-DF protocol. We can see that employing the ISLS approach for the outage SLS-DF protocol can offer the comparable performance to that for the ideal SLS-DF protocol. Although the ISLS approach is not optimized for the outage SLS-DF environment, it can offer very close performance to the OSLS approach.

To see the distributed power-consumption for the proposed BPL approaches, we plot the transmit-power ratio in Fig. 4. It is shown that all curves generally increase with increase of the bit-SNR (or decrease of the noise power), i.e., the relay pays the increasing power consumption. This is because the number of bits/block forwarded by the relay is increased with the noise-power reduction. It is also observed that the transmit-power ratio for the OSLS approach is smaller than that for the ISLS approach. This means that the relay pays less power consumption

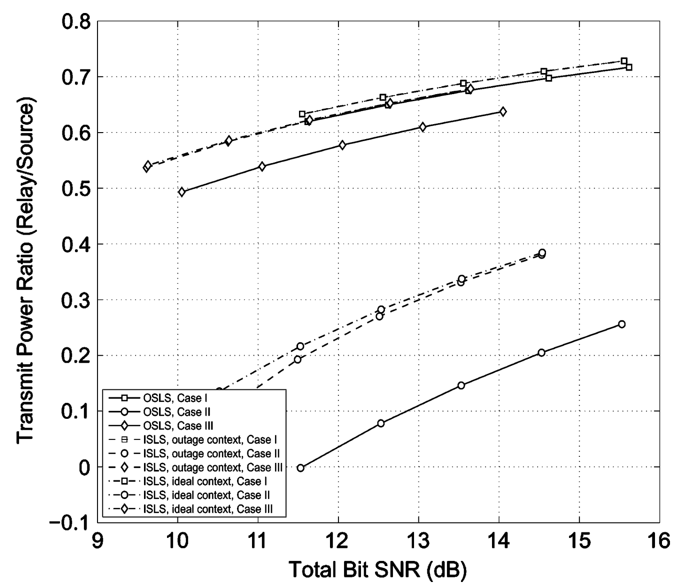

Fig. 4. Transmit Power ratio versus total average bit SNR. A comparison amongst outage SLS-DF, ideal SLS-DF in ideal context, and ideal SLS-DF in outage context.

in the OSLS approach. Another interesting phenomenon is that the relay in Case II expends less power in comparison to other cases. This is because the number of bits/block forwarded by the relay depends on the channel gain for the SR link.

Experiment 2 (SLS-DF, FIPR): This experiment is used to evaluate the proposed FIPR approaches for the outage SLS-DF relaying protocol. The transmit-power ratio between relay and source is set to $\eta = 1$. Fig. 5 illustrates the SER performance for both the ISLS and the OSLS approaches. In contrast to the baselines in Fig. 2, we can see that the proposed approaches offer the significant performance improvement in terms of the SER or the transmit-power per bit. Taking Case I and $\mathcal{P}^{(\mathrm{d})} = 1 \times 10^{-4}$ as an example, both the ISLS and the OSLS approaches outperform the SD-adaptive approach more than 3 dB in terms

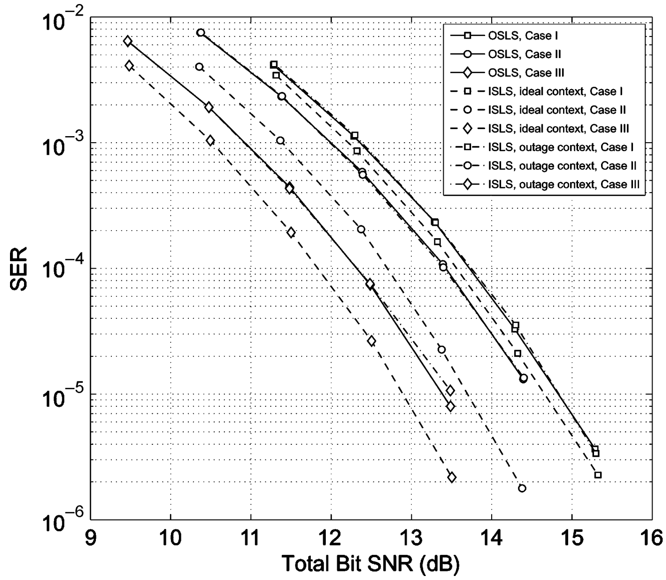

Fig. 5. SER versus total average bit SNR. A comparison amongst outage SLS-DF, ideal SLS-DF in ideal context, and ideal SLS-DF in outage context.

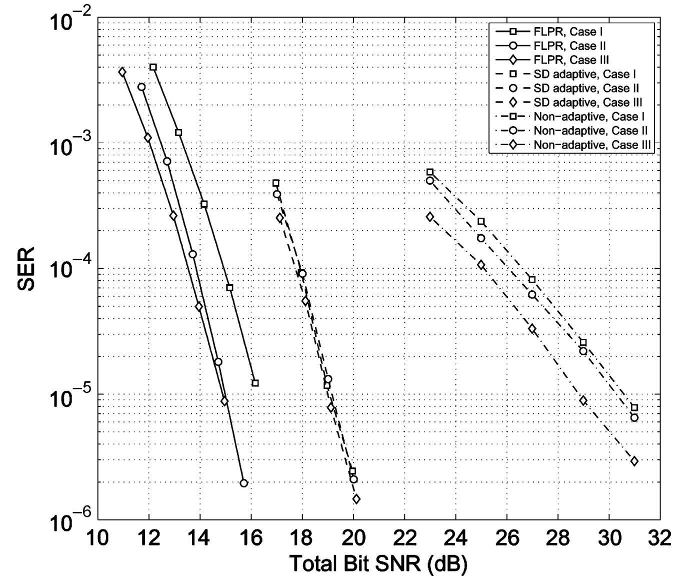

Fig. 6. SER versus total average bit SNR. A comparison amongst FLPR, SD adaptive only, and nonadaptive AF communications.

of the bit-SNR. Although the ISLS approach is originally optimized only for the ideal SLS-DF protocol, its performance in the outage SLS-DF environment is also very close to that for the OSLS approach.

Experiment 3 (SLS-AF, FLPR): The objective of this experiment is to evaluate the proposed FLPR approach for the AF relaying protocol. We first examine the final SER and the total transmit-power efficiency for the proposed approach and plot the results in Fig. 6. It is shown that the proposed approach can significantly improve the SER performance or the transmit-power efficiency. For example Case I and $\mathcal{P}^{(\mathrm{d})} = 1 \times 10^{-4}$, the proposed approach shows around 3 dB and 11 dB gain in comparison with the SD-adaptive approach and the nonadaptive approach, respectively. As for the nonadaptive approach, the transmit-power efficiency for the proposed approach can be further improved when the relay is placed close to the destination (i.e., Case II) or in the middle between the source and the destination (i.e., Case III). However, the performance difference between Case II and Case III is not considerable. We then plot the transmit-power ratio in Fig. 7 to examine the distributed power consumption. It is shown that the transmit-power ratio is almost identical for Cases I and III. The relay in Case II expends less power. It is also observed that all curves generally increase with increase of the bit-SNR (or decrease of the noise power). This is because the transmit-power ratio for the AF protocol is given by $\eta_m = \varepsilon_m^{(\mathrm{r})}/(|h_m^{(\mathrm{sr})}|^2\varepsilon_m^{(\mathrm{s})} + \mathcal{N}_o)$. Obviously, the reduction of noise power can result in the increase of η_m.

Experiment 4 (SLS-AF, FIPR): This experiment is used to evaluate the proposed FIPR approach for the AF-relaying protocol in the local-resource-restriction context. The transmit-power ratio between relay and source is set to $\eta = 1$. Fig. 8 illustrates the SER performance for both the proposed approach and the SD-adaptive approach. The results show that the proposed approach offers the considerable performance improvement in terms of the SER or the total transmit-power efficiency. Taking Case I and $\mathcal{P}^{(\mathrm{d})} = 1 \times 10^{-4}$ as an example, the proposed approach outperforms the SD-adaptive approach

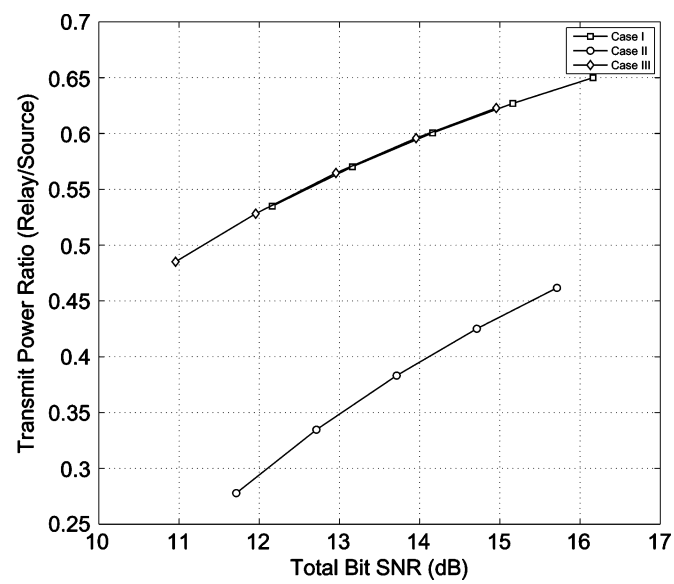

Fig. 7. Transmit Power ratio versus total average bit SNR for the FLPR AF approach.

about 1.5 dB gain. The performance improvement becomes more large for Case II (about 2.5 dB) and Case III (about 3.5 dB).

VI. Conclusion

In this paper, we have investigated the margin-adaptive approaches for the OFDM-based three-node relaying communications, where the orthogonal half-duplex relay could use either the SLS-DF or the AF relaying protocol to retransmit the information. The MRC has been employed at the destination to attain the achievable link performance. With respect to various power-consumption conditions, the proposed approaches have been carefully designed for both the FLPR and the FIPR contexts. Specifically, two BPL approaches, i.e., the ISLS approach and the OSLS approach, have been proposed for the SLS-DF protocols. The ISLS approach was based on the assumption that

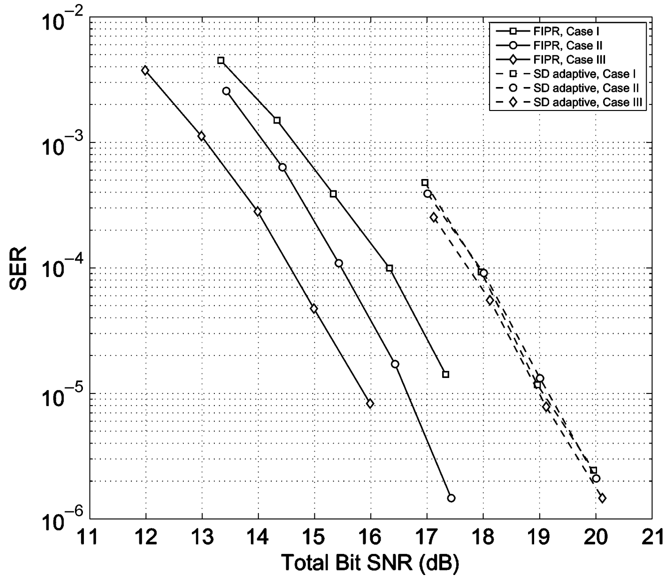

Fig. 8. SER versus total average bit SNR. A comparison between FIPR and SD adaptive case.

the relay could perform the ideal symbol-error detection. The OSLS approach was based on the assumption that the relay only knew the received-SNR for each subcarrier. It has been shown that these two approaches could offer very close performance in the outage SLS-DF protocol. Moreover, the BPL approach has been intensively investigated for the AF relaying protocol. Simulation results have shown that the proposed BPL approaches could significantly improve the performance in terms of the link performance and the transmit-power efficiency.

Appendix A

Proof of the condition for $\min(\xi_2, \mathcal{E}_m) = \xi_2$*:* Suppose $\xi_2 < \mathcal{E}_m$. We should have the following inequality:

$$f(\mathcal{E}_m) = A_m B_m \mathcal{E}_m^2 + 2A_m C_m \mathcal{E}_m + C_m D_m < 0 \quad (61)$$

which can be detailed into

$$\left|h_m^{(\mathrm{sr})}\right|^4 \left(\left|h_m^{(\mathrm{sd})}\right|^2 - \left|h_m^{(\mathrm{rd})}\right|^2\right) \mathcal{E}_m^2 + \left|h_m^{(\mathrm{sr})}\right|^2 \mathcal{N}_o \left(2\left|h_m^{(\mathrm{sd})}\right|^2 - \left|h_m^{(\mathrm{rd})}\right|^2\right) \mathcal{E}_m + \left|h_m^{(\mathrm{sd})}\right|^2 \mathcal{N}_o^2 < 0. \quad (62)$$

It can be easily shown that $f(\mathcal{E}_m) = 0$ has two real roots (denoted by α_1 and α_2), i.e.,

$$\alpha_1 = -\frac{\mathcal{N}_o}{\left|h_m^{(\mathrm{sr})}\right|^2} < 0 \quad (63)$$

$$\alpha_2 = \frac{\left|h_m^{(\mathrm{sd})}\right|^2 \mathcal{N}_o}{\left|h_m^{(\mathrm{sr})}\right|^2 \left(\left|h_m^{(\mathrm{rd})}\right|^2 - \left|h_m^{(\mathrm{sd})}\right|^2\right)}. \quad (64)$$

For the case of $|h_m^{(\mathrm{sd})}| > |h_m^{(\mathrm{rd})}|$, we can see that (62) holds only when $\alpha_2 < \mathcal{E}_m < \alpha_1 < 0$, which is not possible. For the case of $|h_m^{(\mathrm{sd})}| < |h_m^{(\mathrm{rd})}|$, (62) holds only when $\mathcal{E}_m > \alpha_2 > 0$.

Appendix B

Proof of the threshold γ_t*:* Assuming $\xi_1 < \mathcal{E}_m < \xi_t$, we should have

$$\gamma^{(\mathrm{mrc})}\Big|_{\varepsilon_m^{(\mathrm{s})} = \xi_1} > \gamma^{(\mathrm{mrc})}\Big|_{\varepsilon_m^{(\mathrm{s})} = \mathcal{E}_m} \quad (65)$$

which is followed by

$$\frac{\left|h_m^{(\mathrm{sr})}\right|^2 \left|h_m^{(\mathrm{rd})}\right|^2 \xi_1}{B_m \xi_1 + C_m} > \left|h_m^{(\mathrm{sd})}\right|^2. \quad (66)$$

We can easily show $B_m \xi_1 + C_m > 0$, and can rewrite (66) into

$$\underbrace{\left(\left|h_m^{(\mathrm{sr})}\right|^2 \left|h_m^{(\mathrm{rd})}\right|^2 - B_m \left|h_m^{(\mathrm{sd})}\right|^2\right)}_{=-A_m} \xi_1 > C_m \left|h_m^{(\mathrm{sd})}\right|^2. \quad (67)$$

Replacing ξ_1 with

$$\xi_1 = \frac{-2A_m C_m - \sqrt{\Delta_m}}{2A_m B_m} \quad (68)$$

the following inequality can be obtained:

$$\left|h_m^{(\mathrm{sd})}\right|^4 B_m C_m + A_m D_m - 2\left|h_m^{(\mathrm{sd})}\right|^2 A_m C_m < 0. \quad (69)$$

Equations (43) and (46) indicate

$$\left|h_m^{(\mathrm{sd})}\right|^2 C_m = \left(D_m - \left|h_m^{(\mathrm{sr})}\right|^2 \left|h_m^{(\mathrm{rd})}\right|^2 \mathcal{E}_m\right) \quad (70)$$

$$A_m = B_m \left|h_m^{(\mathrm{sd})}\right|^2 - \left|h_m^{(\mathrm{sr})}\right|^2 \left|h_m^{(\mathrm{rd})}\right|^2. \quad (71)$$

Then, the third term at the left hand of (69) can be written into

$$-2\left|h_m^{(\mathrm{sd})}\right|^2 A_m C_m = -A_m \left(D_m - \left|h_m^{(\mathrm{sr})}\right|^2 \left|h_m^{(\mathrm{rd})}\right|^2 \mathcal{E}_m\right) + \left|h_m^{(\mathrm{sd})}\right|^2 \left|h_m^{(\mathrm{sr})}\right|^2 \left|h_m^{(\mathrm{rd})}\right|^2 C_m - B_m C_m \left|h_m^{(\mathrm{sd})}\right|^4. \quad (72)$$

Plugging (72) into (69) results in

$$\left|h_m^{(\mathrm{sd})}\right|^2 C_m + A_m \mathcal{E}_m < 0. \quad (73)$$

We plug (43) and (45) into (73) and obtain

$$\left|h_m^{(\mathrm{sr})}\right|^2 \left(\left|h_m^{(\mathrm{sd})}\right|^2 - \left|h_m^{(\mathrm{rd})}\right|^2\right) \mathcal{E}_m < -\left|h_m^{(\mathrm{sd})}\right|^2 \mathcal{N}_o. \quad (74)$$

We can see that (74) does not hold for $|h_m^{(\mathrm{sd})}| \geqslant |h_m^{(\mathrm{rd})}|$. When $|h_m^{(\mathrm{sd})}| < |h_m^{(\mathrm{rd})}|$, (74) leads to the threshold shown in (55).

Appendix C

Proof of lemma 4: For $A_m < 0$ and $B_m = 0$, (42) results in

$$\varepsilon_m^{(\mathrm{s})} \leqslant -\frac{D_m}{2A_m}, = \frac{\left(\left|h_m^{(\mathrm{sd})}\right|^2 \left|h_m^{(\mathrm{rd})}\right|^2 + \left|h_m^{(\mathrm{rd})}\right|^4\right) \mathcal{E}_m + \left|h_m^{(\mathrm{sd})}\right|^2 \mathcal{N}_o}{2\left|h_m^{(\mathrm{rd})}\right|^4}. \quad (75)$$

Then, $\gamma_m^{(\mathrm{d})}$ achieves the maximum at

$$\varepsilon_m^{(\mathrm{s})} = \min\left(-\frac{D_m}{2A_m},\, \mathcal{E}_m\right). \tag{76}$$

Under the condition $|h_m^{(\mathrm{sd})}| \geqslant |h_m^{(\mathrm{rd})}|$, we can easily obtain

$$-\frac{D_m}{2A_m} \geqslant \frac{2\left|h_m^{(\mathrm{rd})}\right|^2 \mathcal{E}_m + \mathcal{N}_o}{2\left|h_m^{(\mathrm{rd})}\right|^2} > \mathcal{E}_m. \tag{77}$$

In this case, the maximum of $\gamma_m^{(\mathrm{d})}$ is achieved at $\varepsilon_m^{(\mathrm{s})} = \mathcal{E}_m$. For the condition $|h_m^{(\mathrm{sd})}| < |h_m^{(\mathrm{rd})}|$, we let $-(D_m/2A_m) \leqslant \mathcal{E}_m$ and have the result (49).

Acknowledgment

The authors would like to thank the Associate Editor, Prof. Qing Zhao, and anonymous reviewers for the efficient review process and extremely consecutive and supportive comments.

References

[1] J. N. Laneman, D. N. C. Tse, and C. W. Wornell, "Cooperative diversity in wireless networks: Efficient protocols and outage behavior," *IEEE Trans. Inf. Theory*, vol. 50, pp. 3062–3080, Dec. 2004.
[2] A. Nosratinia, T. Hunter, and A. Hedayat, "Cooperative communication in wireless networks," *IEEE Commun. Mag.*, vol. 42, pp. 74–80, Oct. 2004.
[3] T. M. Cover and J. A. Thomas, *Element of Information Theory*, 1st ed. New York: Wiley, 1991.
[4] T. M. Cover and A. A. E. Gamal, "Capacity theorems for the relay channel," *IEEE Trans. Inf. Theory*, vol. 5, pp. 572–584, Sep. 1979.
[5] G. Kramer, M. Gastpar, and P. Gupta, "Coopertive strategies and capacity theorem for relay networks," *IEEE Trans. Inf. Theory*, vol. 51, pp. 3037–3063, Sep. 2005.
[6] D. Chen and J. N. Laneman, "Noncoherent demodulation for cooperative diversity in wireless systems," in *Proc. IEEE Globecom*, Dec. 2004, pp. 31–35.
[7] D. Chen and J. N. Laneman, "Modulation and demodulation for cooperative diversity in wireless systems," *IEEE Trans. Wireless Commun.*, vol. 5, pp. 1785–1794, Jul. 2006.
[8] EU-IST, "Final Report on Identified RI Key Technologies, System Concept, and Their Assessment," IST-2003-507581 WINNER D2.10, Dec. 2005.
[9] EU-IST, Fireworks [Online]. Available: http://fireworks.intranet.gr/main.htm
[10] A. Sendonaris, E. Erkip, and B. Aazhang, "User cooperation diversity-part I: System description," *IEEE Trans. Commun.*, vol. 51, pp. 1927–1938, Nov. 2003.
[11] J. M. Cioffi, Course Notes EE379C- Advanced Digital Communication (Chapter 4) [Online]. Available: http://www.stanford.edu/class/ee379c/
[12] A. Lozano, A. M. Tulino, and S. Verdú, "Optimum power allocation for parallel Gaussian channels with arbitary input distributions," *IEEE Trans. Inf. Theory*, vol. 52, pp. 3033–3051, Jul. 2006.
[13] C. Wong, R. S. Cheng, K. B. Lataief, and R. D. Murch, "Multiuser OFDM with adaptive subcarrier, bit, and power allocation," *IEEE J. Sel. Areas Commun.*, vol. 10, no. 10, pp. 1747–1758, Oct. 1999.
[14] A. M. Wyglinski, F. Labeau, and P. Kabal, "Bit loading with BER-constraint for multicarrier systems," *IEEE Trans. Wireless Commun.*, vol. 4, no. 7, pp. 1383–1387, Jul. 2005.
[15] D. L. Goeckel, "Adaptive coding for time-varying channels using outdated fading estimates," *IEEE Trans. Commun.*, vol. 47, no. 6, pp. 844–855, Jun. 1999.
[16] P. Ormeci, X. Liu, D. L. Goeckel, and R. D. Wesel, "Adaptive bit-interleaved coded modulation," *IEEE Trans. Commun.*, vol. 49, no. 9, pp. 1572–1581, Sep. 2001.
[17] Z. Wang and G. B. Giannakis, "Wireless multicarrier communications: Where Fourier meets Shannon," *IEEE Signal Process. Mag.*, vol. 17, no. 5, pp. 29–48, May 2000.
[18] K. Azarian, H. E. Gamal, and P. Schniter, "On the achievable diversity-multiplexing tradeoff in half-duplex cooperative channels," *IEEE Trans. Inf. Theory*, vol. 51, no. 12, pp. 4152–4172, Dec. 2005.
[19] P. Herhold, E. Zimmermann, and G. Fettweis, "A simple cooperative extension to wireless relaying," in *Proc. IEEE IZSC*, Feb. 2004, pp. 36–39.
[20] A. Adinoyi and H. Yanikomeroglu, "Multi-antenna aspects of wireless fixed relays," in *Proc. IEEE WCNC*, Apr. 2006, pp. 1015–1020.
[21] Z. Yang and L. Tong, "Cooperative sensor networks with misinformed nodes," *IEEE Trans. Inf. Theory*, vol. 51, no. 12, pp. 4118–4133, Dec. 2005.
[22] A. K. Sadek, W. Su, and K. J. R. Liu, "Multinode cooperative communications in wireless networks," *IEEE Trans. Signal Process.*, vol. 55, no. 1, pp. 341–355, Jan. 2007.
[23] S. Lin and D. J. Costello, Jr., *Error Control Coding*. Englewppod Cliffs, NJ: Prentice Hall, 2004.
[24] J. Proakis, *Digital Communications*, 4th ed. New York: McGraw-Hill, 2001.
[25] M. K. Simon and M.-S. Alouini, *Digital Communication Over Fading Channel*, 2nd ed. New York: Wiley, 2005.
[26] J. F. Blowey, A. W. Craig, and T. Shardlow, *Frontiers in Numerical Analysis*. Berlin, Germany: Springer Verlag, 2003.
[27] I. Hammerstrom and A. Wittneben, "On the optimal power allocation for nonregenerative OFDM relay links," in *Proc. IEEE ICC Conf.*, Istanbul, Jun. 2006, vol. 10, pp. 4462–4468.
[28] ETSI, "Broadband Radio Access Networks (BRAN); High Performance Radio Local Area Networks (HIPERLAN) Type 2: Physical Layer," Doc. DTS0023003, France, Dec. 1999.
[29] J. Medbo and P. Schramm, "Channel Models for HIPERLAN/2 in Different Indoor Scenarios," BRAN 3ERI085B, Mar. 1998.

Yi Ma (M'04) is a Postdoctoral Research Fellow at the Centre for Communication Systems Research (CCSR), University of Surrey, Surrey, U.K.

His research interests include network information theory, signal processing advances in wireless communications, coding and communication theory.

Na Yi (S'06) is currently working toward the Ph.D. degree at the Centre for Communication Systems Research (CCSR), University of Surrey, Surrey, U.K.

Her research interests include cooperative relaying, signal processing for communications, network information theory.

Rahim Tafazolli is a Professor of Mobile/Personal communication and Head of Mobile Communications Research Group and is also the Director of Research in the School of EEITM, University of Surrey, Surrey, U.K.

He has been active in research for 20 years and has authored and co-authored more than 300 papers in referred international journals and conferences.

Prof. Tafazolli has been consultants to many mobile companies, lectured and chaired a number of IEE Summer schools and IEEE workshops and conferences. He has carried out many consultancies for mobile companies, Home Office and European Union all in the field of mobile communications. He is the Founder and Chairman of IEE International Conference on 3rd Generation Mobile Communications. He is the chairman of e.Mobility Technology Platform Expert Group tasked with defining strategic research agenda for EU FP7 programme of research on mobile/wireless communications.